Properties of charge recombination in liquid argon

Ettore Segreto[*]

Instituto de Física "Gleb Wataghin" Universidade Estadual de Campinas—UNICAMP Rua Sérgio Buarque de Holanda, No 777, CEP 13083-859 Campinas, São Paulo, Brazil

(Received 1 May 2024; accepted 9 August 2024; published 10 September 2024)

Liquid argon is an excellent medium for detecting particles, given its yields and transport properties of light and charge. The technology of liquid argon time projection chambers has reached its full maturity after four decades of continuous developments and is, or will be, used in world class experiments for neutrino and dark matter searches. The collection of ionization charge in these detectors allows to perform a complete tridimensional reconstruction of the tracks of charged particles, calorimetric measurements, particle identification. This work proposes an innovative approach to the problem of charge recombination in liquid argon which moves from a microscopic model and is applied to the cases of low energy electrons, alpha particles, and nuclear recoils. It takes inspiration and expands the recombination models commonly used by the liquid argon community. The model is able to describe precisely several sets of experimental data available in the literature, over wide ranges of electric field strengths and kinetic energies and can be easily extended to other particles.

DOI: 10.1103/PhysRevD.110.062002

I. INTRODUCTION

Liquid argon (LAr) is used as active medium in several particle detectors [1–9] thanks to its excellent charge and light yields when excited by ionizing radiation [10]. LAr is transparent to its own scintillation light and also allows for the transport of ionization charge over distances up to 10 m under the action of an electric field (typically of the order of 500 V/cm) [11,12]. Charge and light signals are anticorrelated and complementary. The passage of ionizing radiation in LAr produces excited atoms and electron-ion pairs. Two excited argon atoms form the argon excimer Ar_2^* which decays to its ground state emitting a scintillation photon. Ionized atoms recombine with electrons to form excited atoms which then also combine into Ar_2^* and produce scintillation photons. The first channel is often referred to as the excitation one and the second as the recombination one [10]. In the presence of an external electric field a fraction of the ionization charge can be extracted from the production point, drifted toward the anode plane and eventually detected. This reduces the number of scintillation photons emitted through the recombination channel by an amount equal to the number of extracted electrons. The simultaneous detection of scintillation and charge signals is typically extremely useful [13]. Large liquid argon time projection chambers (LArTPC) are used to detect neutrino interactions with energies ranging from few GeV (neutrinos from accelerators, atmospheric neutrinos) down to tens of MeV (Supernova neutrinos, Solar neutrinos) which produce secondary particles with track lengths ranging from several meters to few centimeters or less. Free ionization electrons created by the charged secondary particles are detected on the anode plane by an array of independent, parallel sensing elements (wires or strips) with a pitch of few millimeters. Reading out the signals of all the sensing elements allows us to reconstruct a bidimensional projection of the particles' tracks, while the multiple read-out of the same ionization charge over few (two or three) different planes, with different orientations of the sensing elements, allows to perform a complete tridimensional reconstruction. The detection of the scintillation signal is used to determine the T_0 of the ionizing event, the time at which the electrons are produced and start drifting, that allows to reconstruct the absolute position of the track inside the active volume along the drift coordinate [14] to correct for charge absorption from electronegative contaminants during the drift and eventually fiducialize the active volume. The drift of ionization electrons is a slow process: drift velocity is of the order of 1 mm/μsec at a field of 500 V/cm, while the propagation of photons is much faster [15]. The collected charge allows to perform precise measurements of the dE/dx and of the total deposited energy of each single charged secondary particle produced in a neutrino interaction, that are fundamental tools to identify its flavor and

[*]Contact author: segreto@ifi.unicamp.br

to measure its kinetic energy. Current and next generation LAr neutrino experiments [2,12] can profit of the recent developments in photon detectors with large coverage [16] to exploit also the light signal for calorimetric measurements with a resolution comparable to the charge one.

LArTPC used in low energy experiments (for direct dark matter detection) are smaller than those for neutrinos and are operated in dual phase [4,6,17]. Ionization charge is drifted toward the gas-liquid interface, extracted and accelerated to produce a secondary scintillation signal proportional to the extracted charge. The charge signal is used to localize the event inside the detector, to fiducialize its active volume, for an efficient rejection of external background and to discard multiple events which are incompatible with a dark matter particle interaction. Double phase detectors are able to detect ionization charge with very high efficiency (close to 100%) and down to one single electron, where the scintillation signal is not present. Exploiting ionization only signals allows to lower the detection threshold down to the keV level, which opens the possibility of investigating the existence of light dark matter candidates [18].

Charge recombination is the fundamental process which determines the fraction of ionization electrons that is actually extracted from the production point through the action of an external electric field. The extraction of electrons is referred to their removal from the electronic cloud and not to the extraction in gaseous phase or in other media. Its understanding is essential for any calorimetric measurement based on charge collection. Several theoretical models of electron ion recombination have been formulated along the years [19–21] which have demonstrated to work well just in limited ranges of energies and electric fields due to the approximations they contain about the distribution of the charges, electron and ion diffusion, Coulomb repulsion, …

Many other phenomenological models have been proposed to adjust specific datasets that typically introduce *ad hoc* parameters with limited or no physical meaning [22–24]. More recently and given the impressive evolution of scientific computing, significative advances have been made in the simulation of electron ion recombination in liquid argon [25–28] with encouraging results that elucidate the gross features of the processes involved but that are not yet able to explain the fine details of the dependence on the external electric field and on the ionization densities. This is likely related to the complexity of the problem, to the choices in the modeling of the energy and momentum loss mechanisms and to a number of unknown parameters (track structure, secondary electrons energy distribution, …) which still need to be addressed experimentally.

For these reasons, in this work, a semiempirical approach has been preferred, based on experimental data, with the goal of proposing a common and general approach to the charge recombination problem for different particle types, kinetic energies and in a wide range of external electric field intensities. The proposed microscopic model is applied to the different cases on the basis of general physical considerations about the track structure and the distribution of the electronic cloud around the positive ions.

II. RECOMBINATION MODEL

A charged particle moving inside a LAr volume produces an equal amount of ionization electrons and positive ions. The application of an external electric field, $\mathcal{E}$, allows to extract a fraction of the negative charge from the production region that can be eventually detected, while the ions go typically undetected because their drift velocity is three orders of magnitude smaller [29]. The other fraction of negative charge recombines with ions, resulting in the emission of scintillation photons.

From a microscopic point of view, the infinitesimal amount of charge dq, extracted from an infinitesimal energy deposition dE, can be written as

$$dq = dq_i \times P(\mathcal{E}, dq_i/dx, Q_i, \ldots) \tag{1}$$

where $dq_i = dE/w_i$ is the ionization charge produced (positive and negative), w_i is the energy needed to produce an electron ion pair and P is the probability of extracting the ionization electrons from the production point through the action of an external electric field $\mathcal{E}$. P can be a function of the linear ionization density dq_i/dx or of the total ionization charge Q_i, depending on the particle type and its kinetic energy. The extraction probability is written in the general form

$$P = \frac{\mathcal{E}^\alpha}{\mathcal{E}_{1/2} + \mathcal{E}^\alpha} \tag{2}$$

where $\mathcal{E}$ is the external electric field per kV/cm and $\mathcal{E}_{1/2}$ and α are two parameters. In particular $\mathcal{E}_{1/2}$ sets the value that $\mathcal{E}^\alpha$ needs to reach to extract 50% of the ionization charge. For uniformity with $\mathcal{E}$, it is assumed that $\mathcal{E}_{1/2}$ has the dimensions of an electric field per kV/cm.

Consistently with [24], the recombination factor, R, is defined as

$$R = \frac{1}{Q_i}\int_0^{Q_i} dq \tag{3}$$

where dq is given by Eq. (1) and Q_i is the total number of free electrons produced by the ionizing particle in LAr. The factor R represents the fraction of ionization electrons which is extracted from the production point. Another quantity which is often used in place of the recombination factor is the charge yield, Q_Y, defined as:

$$Q_Y = \frac{1}{E_{\text{kin}}}\int_0^{Q_i} dq \tag{4}$$

that gives the number of electrons extracted per unit of energy deposited in LAr.

III. CHARGE RECOMBINATION FOR ELECTRONIC RECOILS

The ICARUS and ARGONEUT Collaborations have shown that the local recombination process for stopping protons and muons, over a broad range of electric fields and LET, can be well described by Eqs. (1) and (2), with $\alpha = 1$, $\mathcal{E}_{1/2} = k\frac{dq_i}{dx}$ and w_i constant [24,30]. The extraction probability can be written, in this case, as

$$P = \frac{\mathcal{E}}{k\frac{dq_i}{dx} + \mathcal{E}} \tag{5}$$

This can be considered an appropriate description for tracks with a cylindrical symmetry. A plausible derivation of Eq. (5) is given in Appendix A, where it is also shown how the parameter k can be related to the radius, r_0, of the cylindrical electronic cloud as follows:

$$k = \frac{e}{2\pi\epsilon_{LAr} r_0} \tag{6}$$

where e is the electron charge and ϵ_{LAr} is the dielectric constant of liquid argon.

In this work it is assumed that the track geometry for electronic recoils with energies between 1 MeV and few keV is cylindrical and that the extraction probability is described by Eq. (5).

Below 1 MeV, the energy deposited in LAr by the primary electron is entirely transferred to the electrons of the medium and w_i is found to be constant down to few tens of keV [23] and to have a value of $w_i = 23.6$ eV [31]. The energy loss of electrons in this range of energies is well described by [32]:

$$\frac{dE}{dx} \simeq \frac{\alpha_e}{E} + \beta_e \tag{7}$$

with $\alpha_e = 0.227 \pm 0.007$ MeV^2/cm and $\beta_e = 1.7 \pm 0.1$ MeV/cm. Substituting Eq. (7) in Eq. (5) and integrating Eq. (3) between zero and the initial energy of the incoming electron, E_{kin}:

$$R = \frac{\mathcal{E}}{\mathcal{E} + \frac{k}{w_i}\beta_e}\left[1 - \frac{\log(1+z)}{z}\right] \tag{8}$$

where z is defined as

$$z = \frac{\mathcal{E} + \frac{k}{w_i}\beta_e}{\frac{k}{w_i}\alpha_e} E_{\text{kin}} \tag{9}$$

A. Escaping electrons

It is reported in the literature that for lightly ionizing particles (electrons, muons) a fraction of the free electrons escapes the recombination with positive ions, even in the absence of an external electric field [33,34]. The effect is inversely proportional to the LET, since for more heavily ionizing particles it is not observed [35]. In presence of escaping electrons the extraction probability, P_e, can be written as

$$\begin{aligned} P_e &= (1 - S(dq_i/dx)) \times P + S(dq_i/dx) \\ &= P + S \times (1 - P) \end{aligned} \tag{10}$$

where $S(dq_i/dx)$ is the fraction of free electrons that escapes recombination and that does not depend on the electric field $\mathcal{E}$ and P is defined in Eq. (5). Consistently with Eq. (5), the escaping probability is written as

$$S = \frac{1}{1 + \frac{dq_i/dx}{\gamma}} \tag{11}$$

where γ is a parameter. If $\frac{dq_i/dx}{\gamma}$ is much greater than one, Eq. (11) can be approximated with

$$S \simeq \frac{\gamma}{dq_i/dx} \tag{12}$$

This approximation does not lead to singularities in S, since dq_i/dx is always grater then zero [36]. The second term in Eq. (10) can be written as

$$S(1 - P) \simeq \frac{k\gamma}{k\frac{dq_i}{dx} + \mathcal{E}} \tag{13}$$

and the recombination factor of Eq. (8) needs to be slightly modified into

$$R_e = R \times E_e \tag{14}$$

where

$$E_e = 1 + \frac{k\gamma}{\mathcal{E}} \tag{15}$$

R_e depends on two parameters: k and γ, that can be estimated through the comparison with data.

Three datasets are considered to retrieve these two parameters: Scalettar *et al.* [37], with electrons from a ^{113}Sn source (364 kev), Aprile *et al.* [38] with electrons from a ^{207}Bi source (976 keV) and Ereditato *et al.* [39] with Compton electrons from the scattering of gammas from a ^{60}Co source (1,173 MeV and 1,332 MeV).

The result of the fit of Scalettar dataset with Eq. (14) is shown in Fig. 1. An additional multiplicative constant has

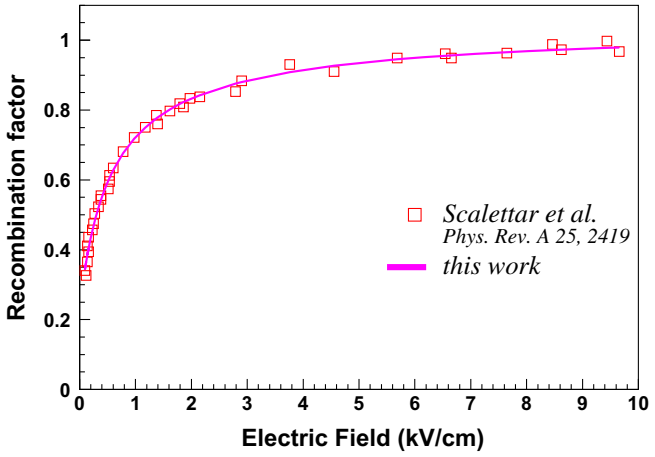

FIG. 1. Fit of the Scalettar data sample [37] with Eq. (14). Electrons are produced by a ^{113}Sn source with an energy of 364 keV.

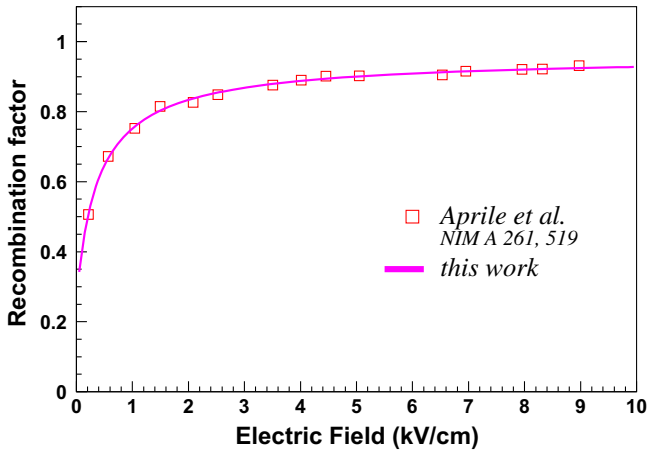

FIG. 2. Fit of the Aprile data sample [38] with Eq. (14). Electrons are produced by a ^{207}Bi source with an energy of 976 keV.

been included in the fit to take into account possible systematic effects on the normalization of the experimental points. The fit returns a value of $1,04 \pm 0,01$ for this multiplicative constant. The result of the fit of Aprile dataset with Eq. (14) is shown in Fig. 2. Also in this case an additional multiplicative constant is considered and the fit returns a value of $0.96 \pm 0,01$. Finally, the result of the fit of Ereditato dataset is shown in Fig. 3 and the value of the multiplicative constant is $1.02 \pm 0,01$.

The three sets of parameters obtained with the fitting procedures are reported in Table I. The model describes the experimental points very well, along the entire range of electric fields and the three sets of parameters are well compatible within errors. A simultaneous fit of the three sets of data has also been performed and the result is reported in Table I.

An additional dataset has been used to test this model and the result of the fit is shown in Appendix B. The data

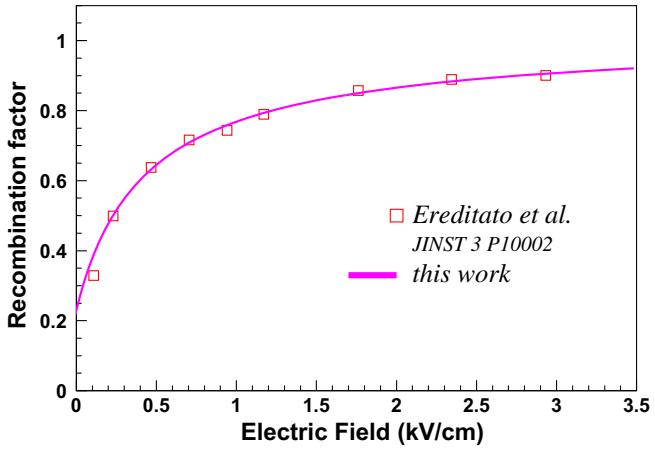

FIG. 3. Fit of the Ereditato data sample [39] with Eq. (14). Electrons are produced by the Compton scattering of gammas emitted by a ^{60}Co source with energies of 1.173 MeV and 1.332 MeV. The electrons with energies corresponding to the endpoint of the Compton spectrum are used to produce the plot.

come from the recoil directionality (ReD) experiment [23] and the electrons are produced through the conversion of γ rays from a ^{241}Am source.

Using the approximate value of $k = 4$ mV and inverting Eq. (6), it is possible to estimate a value of $r_0 \simeq 500$ nm.

B. Electrons–LAr doped with nitrogen

An interesting set of measurements of charge recombination in LAr doped with different levels of nitrogen [40] allows to test the hypotheses of the model about the dependence of the recombination parameter k on the radial extension of the electronic cloud. Nitrogen molecules present a series of vibrational states which can absorb the energy of the secondary electrons much more efficiently than pure LAr. The thermalization length of secondary electrons produced by the conversion of 1.7 MeV x-rays in liquid nitrogen (LN_2) has been extensively studied by Ramanan and Freeman [41] also as a function of the density of the liquid, from 467 kg/m^3 up to 809 kg/m^3. The thermalization length decreases exponentially with increasing density up to ≃590 kg/m^3 where it reaches a

TABLE I. Parameters k and γ obtained with the fit of the Scalettar dataset—e^- of 364 keV [37]—of the Aprile dataset—e^- of 976 keV [38]—with Eq. (14)—and of Ereditato dataset—e^- of 1.004 MeV [39]. The values of the parameters obtained with a simultaneous fit of the three datasets are also reported.

	Energy (keV)	k (mV)	γ (μm^{-1})
Scalettar	364	3.9 ± 0.2	3.0 ± 0.2
Aprile	976	3.7 ± 0.3	2.8 ± 0.3
Ereditato	1004	4.2 ± 0.4	2.3 ± 0.5
All		$\mathbf{3.8 \pm 0.2}$	$\mathbf{2.8 \pm 0.2}$

plateau. The behavior at low densities is attributed to electron detachment and migration by hopping or by a two state mechanism [42], while at higher densities this process is truncated by electron capture to form an anion. Assuming that a similar mechanism is active in nitrogen doped LAr, the radial extension of the electronic cloud produced by an electronic recoil should decrease exponentially with the nitrogen concentration and consequently the parameter k increase exponentially with the same rate, as suggested by Eq. (6). Data from [40] are taken over a wide range of electric field strengths and for eight different concentrations of nitrogen in LAr ($[N_2]$): 1%, 3%, 5,6%, 6,4%, 7,9%, 9,9%, 12,4%, 14,9% and pure LAr. For any given $[N_2]$, experimental data are fitted with Eq. (14), where the $\gamma_{[N_2]}$, for the escaping electrons, and the $w_{[N_2]}$, for the energy spent per electron ion pairs, are left as free independent parameters, while the parameters $k_{[N_2]}$ are constrained to follow the relation

$$k_{[N_2]} = k_0 \exp(h[N_2]) \tag{16}$$

where k_0 and h do not depend on $[N_2]$. The fit returns a value of $h = 20,8 \pm 0,4$; $w_{[N_2]}$ increases from the nominal value of 23.6 eV for pure LAr to ≃39.0 eV for 14,9% of nitrogen, which implies the existence of some quenching mechanism at the production stage of the free charge; $\gamma_{[N_2]}$ goes to zero for concentrations above 3%. The result of the fit is shown in Fig. 4. The model describes the experimental data well and the dependence of the $k_{[N_2]}$ on $[N_2]$ is reproduced correctly.

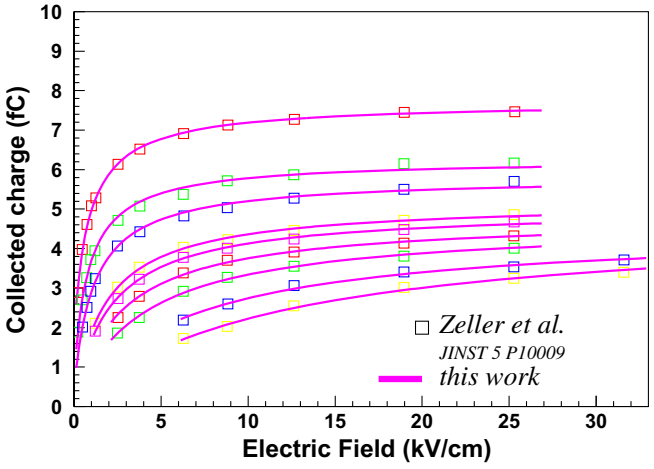

FIG. 4. Fit of the Zeller data sample [40]. Electrons are produced by the Compton scattering of gammas from a ^{60}Co source. Data are taken with LAr doped with nitrogen at several different concentrations. Increasing nitrogen concentration produces an overall quenching of the free charge and a visible change of the parameters $k_{[N_2]}$ that determine the slope of the curves of the collected charge as a function of the applied electric field. From top to bottom, the data points correspond to: pure LAr, 1%, 3%, 5,6%, 6,4%, 7,9%, 9,9%, 12,4%, 14,9% of $[N_2]$. Squares of the same color refer to the same level of $[N_2]$. Magenta lines represent the result of the fitting procedure described in the text.

C. Electrons–low energy limit

At higher energies, the distribution of positive and negative charges produced by the primary electron has an approximately cylindrical symmetry and the extraction probability is described by Eq. (5). When the energy of the primary electron drops below a certain limit, the spatial extension of the free electrons' cloud exceeds the length of the positive ions' track and takes an approximately spherical shape. In this limit, the extraction probability depends only on the total amount of positive and negative charge produced by the primary electron and not on the details of dQ/dx along the track and it is necessary to define $\mathcal{E}_{1/2} = k_l Q_i = k_l \frac{E_{kin}}{w_i}$. The extraction probability is written as

$$P^l = \frac{\mathcal{E}}{k_l Q_i + \mathcal{E}} \tag{17}$$

A derivation of Eq. (17) is reported in Appendix A. Also in this case, the parameter k_l can be related to the size of the electronic cloud

$$k_l = \frac{e}{4\pi\epsilon_{LAr} r_0^2} \tag{18}$$

where r_0 is the radius of the spherical negative charge distribution (see Appendix A for more details). Eq. (10) for escaping electrons continues to be valid, but, consistently with Eq. (17), S^l needs to be defined as

$$S^l = \frac{1}{1 + \delta \times Q_i} \tag{19}$$

where δ is a parameter. It is not possible to make the same approximation as in the high energy case, since Q_i tends to zero when the energy of the primary electron goes to zero.

The recombination factor, R^l, is obtained substituting Eq. (17) into Eq. (3), remembering that no integration is needed and using Eq. (19)

$$R^l = \frac{\mathcal{E}}{k_l Q_i + \mathcal{E}} \times \left[1 + \frac{k_l Q_i / \mathcal{E}}{1 + \delta \times Q_i}\right] \tag{20}$$

The transition between the high and low energy regimes happens when the primary electron has a kinetic energy of few keV. The range of an electron with kinetic energy E_0 can be written as

$$X = \int_0^{E_0} \frac{dx}{dE} dE = \frac{E_0^2}{2\alpha_e} \tag{21}$$

where Eq. (7) has been used and the parameter β_e has been neglected. The boundary between the two regimes is

reached when the range X is of the order of two times the radius of the cylindrical charge distribution, estimated through Eq. (6). Hence

$$E_{bd} = \sqrt{4\alpha_e r_0} \simeq 7 \text{ keV} \tag{22}$$

where the value of 500 nm for r_0 has been used.

D. Electrons–transition region

The most straightforward way to parametrize the transition between low and high energy regimes is to assume that the first one is dominating below a certain energy value, E_{bd}, and the other is dominating above it. In this case, the recombination factor is given by Eq. (20) for $E_{\text{kin}} < E_{bd}$, while for $E_{\text{kin}} > E_{bd}$, by

$$R = \left[R^l(E_{bd}) - R^h(E_{bd})\right] \frac{Q_{bd}}{Q_i} + R^h \tag{23}$$

where R^l is the recombination factor in the low energy limit, R^h the recombination factor in the high energy limit, $Q_{bd} = E_{bd}/w_i$ and $Q_i = E_{\text{kin}}/w_i$.

An interesting set of data that can allow to estimate the values of the parameters k_l, δ, and E_{bd} is the one collected by the DarkSide Collaboration for the charge yield of low energy electron recoils, with energies below 20 keV and shown in Fig. 2 of [22]. Data of charge yield are converted into collected charge and then fitted with $R \times E_{\text{kin}}/w_i$, where R is given by Eq. (23). The fit is almost insensitive to the value of the parameter γ and it has been fixed to 2.9 μm^{-1}. Two separate fits have been performed: one leaving w_i as a free parameter and the other fixing it at the reference value of 23.6 eV. The values of the parameters k_l, δ, and E_{bd} obtained with the two fitting procedures are shown in Table II. The parameter k_h, for the high energy part, returns, in both cases, a value of ~2.0 mV. This is a factor two smaller than what reported in Table I and the discrepancy can be easily attributed to the assumption made about the sharp transition between the low and high energy regimes. The result of the fit is only slightly better when w_i is left as a free parameter and the value returned is consistent with what found by the DarkSide Collaboration —$18,3 \pm 2,5$ eV. The result of the fit is shown in Fig. 5, where only the case with w_i as a fixed parameter is reported, since the other one is just slightly different. Consistently with what predicted by Eq. (22), E_{bd} is found to be in the range of ~10 keV. Inverting Eq. (18) and substituting the value of k_l, it is possible to estimate the radius of the spherical charge distribution, which results to be of the order of 700 nm—not too far from the radius of the cylindrical distribution predicted by Eq. (6).

TABLE II. Parameters k_l, δ, and E_{bd} estimated with the fit of the DarkSide dataset [22] with the model described in the text.

w_i (eV)	k_l (V/cm)	δ	E_{bd} (keV)
16.5 ± 1.5	4.6 ± 0.1	$(8.7 \pm 0.1) \times 10^{-4}$	10.9 ± 0.3
23.6	3.7 ± 0.1	$(9.7 \pm 0.1) \times 10^{-4}$	9.8 ± 0.2

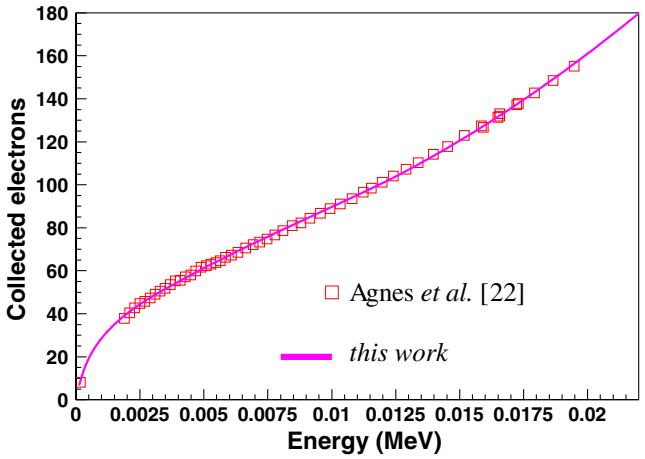

FIG. 5. Number of collected electrons at 0.2 kV/cm for electronic recoils with energies below 20 keV. Charge yields measured in [22] are multiplied by E_{kin} to obtain the number of electrons. The magenta line represents the result of the fit with the parameter w_i set at the value of 23.6 eV (see text).

IV. CHARGE RECOMBINATION FOR NUCLEAR RECOILS

Nuclear recoils with energies below 100 keV produce ionization tracks shorter than approximately 200 nm [43]. Since the kinetic energy of the ionization electrons depends only weakly on the energy of the recoiling particle [28], it is reasonable to assume that the electronic cloud of a nuclear recoil, at thermalization, has a spatial extension comparable to the one of an electronic recoil and thus in the range of several hundreds of nm. It seems appropriate to use the approximation of an electronic cloud with a spherical symmetry, similarly to the case of low energy electrons discussed in Sec. III C.

A relevant difference with respect to electrons is that the speed of the recoiling nucleus ($E_{\text{kin}} \leq 100$ keV) is significantly smaller than that of the ionization electrons when they are emitted ($E_{\text{kin}} \sim 10$–20 eV). The dynamics of the recombination process results to be much more complicate: dividing up the total deposited charge, Q_i, into elementary depositions dq_i and assuming that for each one of the dq_i the ionization electrons are emitted simultaneously, the electronic cloud tends to pile-up into a sort of an onion structure made of overlapped shells, each one containing the same amount of charge dq_i. Each dq_i feels the electric field of the entire positive ions' track, screened by the innermost shells, each one containing an equal amount of charge, dq_i. These considerations lead to a definition of $\mathcal{E}_{1/2}$ which depends on the residual energy of the recoiling nucleus and in particular $\mathcal{E}_{1/2} = k_n q_i$. The extraction probability for nuclear recoils is written as

$$P^n = \frac{\mathcal{E}\ f(\mathcal{E})}{k_n\ q_i + \mathcal{E}\ f(\mathcal{E})} \tag{24}$$

where $f(\mathcal{E})$ is a function which parametrizes the possible effect of the dynamics of the electronic cloud expansion on the extraction probability and k_n is a parameter which depends on the size of the electronic cloud at thermalization. Assuming for $f(\mathcal{E})$ a form of the type $f(\mathcal{E}) = (a\,\mathcal{E})^b$, with $a \to 1$ and $b \to 0$ in the case of no distortion, Eq. (1) can be written

$$dq = dq_i \times \frac{1}{\frac{k_n q_i}{\mathcal{E}^\alpha} + 1} \tag{25}$$

where $\alpha = 1 + b$ and the parameter a^b is absorbed by k_n.

Substituting Eq. (25) into Eq. (3) and integrating between zero and the total amount of charge produced by the nuclear recoil, Q_i, it is possible to obtain the recombination factor:

$$R^n = \frac{1}{z_n}\log(1 + z_n) \tag{26}$$

where

$$z_n = \frac{k_n Q_i}{\mathcal{E}^\alpha} \tag{27}$$

and

$$Q_i = \int_0^{E_{\rm kin}} \frac{dE_i}{w_i} \tag{28}$$

where dE_i is the infinitesimal amount of energy that the nuclear recoil transfers to the electrons of argon atoms. Equation (28) takes into account the possibility that w_i depends on the ionization density of argon.

Recoiling argon nuclei lose a relevant fraction of their kinetic energy through elastic collisions with other nuclei. Lindhard theory [44] predicts the amount of energy transferred to the electrons in terms of the dimensionless variable ε

$$\varepsilon = C_\varepsilon E = \frac{a_{TFF} A_2}{Z_1 Z_2 e^2 (A_1 + A_2)} E \tag{29}$$

where E is the recoil energy, Z and A are the atomic and mass number of the projectile (1) and of the medium (2) and

$$a_{TFF} = \frac{0.8853 a_B}{\left(Z_1^{1/2} + Z_2^{1/2}\right)^{2/3}} \tag{30}$$

$a_B = \hbar/m_e e^2 = 0.529$ Å is the Bohr radius. For $Z_1 = Z_2$ Eq. (29) gives $C_\varepsilon = 0.01354\ \text{keV}^{-1}$. The amount of energy transferred to the electrons of the medium is given by [45]

$$\eta(\varepsilon) = 0.427\varepsilon^{1.193} \tag{31}$$

and dE_i can be written as

$$dE_i = \frac{d\eta(\varepsilon)}{d\varepsilon} dE \tag{32}$$

A possible parametrization of the w_i dependence on the density of ionization energy can be written as

$$w_i = w_i^0 + cE^d \tag{33}$$

where w_i^0 is the limit value for lightly ionizing particles. The recombination model for nuclear recoils depends on five parameters: k_n, α, w_i^0, c, and d. They are estimated through a fit of the dataset collected by the SCENE Collaboration for nuclear recoils of energies between 16.9 and 57.3 keV and for electric fields up to about 0.6 kV/cm [46]. The data are given in terms of charge yield and are fitted with the function

$$Q_y^n = \frac{\mathcal{E}^\alpha}{k_n E_{\rm kin}} \log(1 + z_n) \tag{34}$$

where Eq. (28) is integrated numerically and substituted into Eq. (27). The fit points to a value of $c = 0$ and w_i^0 around 24 eV, disfavoring a dependence of w_i on the energy of the recoiling argon nucleus. This result allows us to simplify the model and to reduce the number of parameters to three: k_n, α, and w_i^0. The total amount of ionization charge becomes

$$Q_i = \frac{\eta(\varepsilon)}{w_i^0 C_\varepsilon} = \frac{0.427 \times (C_\varepsilon E_{\rm kin})^{1.193}}{w_i^0 C_\varepsilon} \tag{35}$$

The result of the fit of the experimental points with the simplified model ($w_i = w_i^0$) is shown in Fig. 6. The values of the parameters coming from the fitting procedure are shown in Table III.

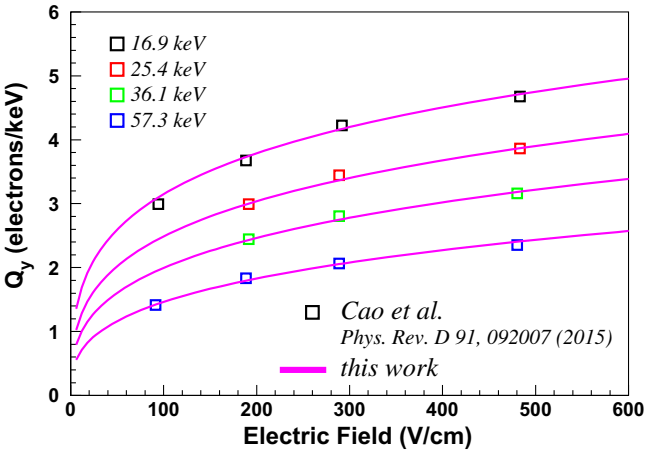

FIG. 6. Charge yield for nuclear recoils with energies ranging from 16.9 keV to 57.3 keV as a function of the applied electric field [46]. Error bars have not been reported since they are very small. Magenta lines represent the result of the fit with the simplified model (w_i^0 kept constant).

TABLE III. Parameters k_n, α, and w_i^0 estimated with the fit of the nuclear recoils' dataset coming form [46] with the model described in the text.

k_n (V/cm)	α	w_0^i (eV)
$(3.7 \pm 0.1) \times 10^{-1}$	0.44 ± 0.02	24.1 ± 0.9

The parameter k_n is exactly one order of magnitude smaller than the corresponding parameter k_l for low energy electrons. The existence of the function $f(\mathcal{E})$ prevents from inferring the radial dimension of the electronic cloud from k_n in a general way, but in the case that a^b were not too different from one, Eq. (18) would imply that it is approximately three times larger than that of a low energy electronic recoil and in the range of few μm. This size would be consistent with the thermalization length predicted by simulations of the electron ion recombination process for nuclear recoils [26].

V. CHARGE RECOMBINATION FOR ALPHA PARTICLES

Alpha particles with a kinetic energy of few MeV have a range in LAr of tens of μm. Assuming that the size of the electronic cloud at thermalization is of the order of 1 μm, as in the case of low energy electrons and nuclear recoils, it seems plausible that it takes a cylindrical symmetry around the positive ions' core [47]. Almost the entire kinetic energy of the α is transferred to the electrons of LAr [48] and the stopping power coincides with its LET. For $E > E_{\max}$ the stopping power can be well approximated by the following formula:

$$\left(\frac{dE}{dx}\right)_{he} \simeq \frac{A}{E + E_0} + B \tag{36}$$

where $E_{\max} = 0.62$ MeV is the kinetic energy which corresponds to the maximum value of the stopping power, $A = 2180$ MeV^2/cm, $E_0 = 1.65$ MeV and $B = 53$ MeV/cm. For $E < E_{\max}$ the stopping power grows logarithmically from zero up to its maximum value. In this case, in order to obtain a fully analytic expression of the extracted charge, a linear approximation is used

$$\left(\frac{dE}{dx}\right)_{le} \simeq C \times E \tag{37}$$

where the parameter $C = 1635$ cm^{-1} is fixed by the constrain that the low and high energy approximations need to give the same value of stopping power for $E = E_{\max}$. The subscripts *he* and *le* stand for *high energy* and *low energy* approximation respectively.

The total extracted charge, Q_a, is obtained by integrating Eq. (1) from zero up to the alpha initial kinetic energy, $E_{\rm kin}$, with an extraction probability given by

$$P = \frac{\mathcal{E}^\alpha}{\frac{k_a}{w_i}\frac{dE}{dx} + \mathcal{E}^\alpha} \tag{38}$$

The integral is split into two parts: the first one from zero up to $E_{\max}$, where Eq. (37) is used for the stopping power and the second from $E_{\max}$ up to $E_{\rm kin}$, where Eq. (36) is used. The extracted charge results to be

$$Q_a = \eta_1 \frac{\log(1 + z_0)}{z_0} + \eta_2 \left[1 - \frac{\log(1 + z_1)}{z_2}\right] \tag{39}$$

where

$$\eta_1 = \frac{E_{\max}}{w_i}, \qquad \eta_2 = \frac{E_{\rm kin} - E_{\max}}{w_i} \frac{\mathcal{E}^\alpha}{\mathcal{E}^\alpha + \frac{k_a B}{w_i}} \tag{40}$$

and

$$z_0 = \frac{k_a\, C\, E_{\max}}{\mathcal{E}^\alpha\, w_i} \tag{41}$$

$$z_1 = \frac{E_{\rm kin} - E_{\max}}{\frac{A\, k_a/w_i}{k_a\, B/w_i + \mathcal{E}^\alpha} + E_0 + E_{\max}} \tag{42}$$

$$z_2 = \frac{E_{\rm kin} - E_{\max}}{\frac{A\, k_a/w_i}{k_a\, B/w_i + \mathcal{E}^\alpha}} \tag{43}$$

The model depends on two parameters: k_a and α, while w_i is set to the reference value of 23.6 eV. Escaping electrons are not considered for alpha particles. Equation (39) could be simplified by letting $E_{\max} \to 0$ so that $\eta_1 = 0$ and only

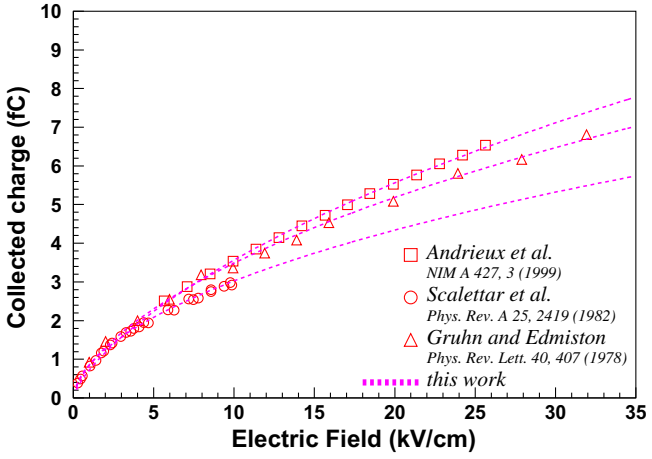

FIG. 7. Extracted charge from alpha recoils. In all three cases alpha particles are produce by ^{241}Am decays in LAr. Experimental points have been separately fitted with Eq. (39).

TABLE IV. Parameters k_a and α extracted through the fitting procedure of the three datasets of α recoils. The parameter w_i is set to 23.6 eV.

	k_a (mV)	α
Scalettar *et al.*	2.3 ± 0.1	0.60 ± 0.01
Gruhn and Edmiston	2.3 ± 0.1	0.67 ± 0.01
Andrieux *et al.*	2.6 ± 0.1	0.76 ± 0.01

the second term survives. Also z_1 and z_2 should be modified accordingly. This simplification gives an approximate value of Q_α accurate at the level of 10% for kinetic energies of the alphas of the order of 5 MeV, since $E_{max} = 0.62$ MeV. The values of the parameters on which the model depends can be determined through a fitting procedure of the data available in the literature. Three sets of data are used, all collected with α particles produced by ^{241}Am, hence with an initial kinetic energy of ~5.5 MeV: Scalettar *et al.* [37], Gruhn and Edmiston [49], and Andrieux *et al.* [50].

The three sets span a very broad range of electric field strengths, up to about 30 kV/cm and are all obtained with small drift chambers with anode to cathode distances of the order of one cm and where the alpha source is directly placed on the cathode. The trends of the extracted charge as a function of the electric field strength do not perfectly overlap and this can be due to different systematic effects on the charge calibration of the read-out systems, degree of purity of the LAr and/or space charge effects. For this reason, experimental points have been fitted separately with Eq. (39) and the results of the fits are shown in Fig. 7, while the best fit values are reported in Table IV.

The model describes well the experimental points along the entire range of electric field strengths. The values of k_a are compatible among them, while the values of α show variations at the level of 20%–25% which descend from the different trends of the data points for electric field strengths above 5 kV/cm.

Below this threshold, that is the most relevant in the vast majority of experimental situations, data and fit functions do not exhibit significant differences.

k_a is not too far from the value of the analogous parameter found for electrons and reported in Table I. This means that the size of the electronic cloud produced by alphas is not too different from that of electrons, since the entity of the distortion discussed for Eq. (24), is probably small, given that the parameter α is reasonably close to one.

VI. DISCUSSION

The model proposed in this work is based on the hypothesis that the charge recombination process can be treated adopting an infinitesimal, local approach which accounts for the details of the track structure in terms of LET and of the electronic cloud configuration at thermalization. This is relevant at low energies, where the LET depends heavily on the kinetic energy of the recoiling particle and approaches based on average values can fail. At higher energies, when the LET of the ionizing particle is almost constant and the electron cloud has a cylindrical symmetry, the model reduces to the so called Doke-Birks phenomenological model [24]. The value of the parameter k, found for electrons with energy below 1 MeV, is around 4 mV and it can be directly compared with the analogous parameter found by the ICARUS and ARONGEUT Collaborations [24,30] for stopping protons and muons, which results to be around 1 mV. The factor four difference could be explained by the production of energetic secondary electrons that result in an increased transversal size of the electronic cloud around the positive ion core and of the positive ion core itself with respect to low energy electrons.

The recombination factor for nuclear recoils, R^n, shown in Eq. (26), is formally identical to the prediction of the (modified) box model [21], while the meaning of the parameters and the hypotheses are different. In the proposed model the extension of the positive ions' distribution is considered to be small with respect to the electronic cloud and the recombination is attributed to their electrostatic interactions at thermalization, while in the box model, positive ions and electrons are uniformly distributed inside a box.

In the case of nuclear recoils ($E < 100$ keV) and of low energy electrons ($E < 10$ keV), it is not expected any dependence of the recombination factor on the mutual orientation of the external electric field and the recoiling nucleus track, since the electronic cloud has an approximately spherical symmetry around the positive ions' core.

The ARGONEUT Collaboration did not observe any significant dependence of the recombination factor for stopping protons on the orientation of the external electric field, of 481 V/cm, with respect to the ionizing track for angles between 80 and 40 degrees [30]. A similar behavior is expected for alpha particles and electrons of higher energy ($E < 1$ MeV) that present a cylindrical symmetry of the electronic cloud which should be similar to the one of stopping protons. This could be due to a rearrangement of the electronic cloud that tends to align the local field, internal to the track, to the external electric field while keeping unchanged the charge density along the same direction. Experimental tests of directional effects in these cases are extremely challenging since the length of the ionization tracks are on the submillimeter scale.

VII. CONCLUSIONS

A microscopic model is developed to describe the charge recombination process in LAr which also includes the effect of escaping electrons for low ionizing particles. The recombination factor for electronic recoils with energies below 1 MeV is calculated through an analytical integration of the model and a fitting procedure of three independent datasets: Scalettar *et al.* [37], Aprile *et al.* [38], and

Ereditato *et al.* [39], allows to estimate the two parameters, k and γ, on which it depends. The three independent fits point to values which are well compatible within errors. For low energy electron recoils the structure of the free electrons' cloud cannot be assumed more as cylindrical, since its dimensions exceeds the length of the core of positive ions and a spherical approximation is more appropriate. The different distribution of the charges leads to a dependence of the recombination factor on the total deposited charge instead of the linear charge deposition. A fit of a dataset from the DarkSide collaboration [22] allows to estimate the limit between the two regimes, which is found to be around 10 keV. The model makes an hypothesis on the dependence of the parameter k on the radial extension of the electronic cloud at thermalization, which is tested with a set of data collected by Zeller *et al.* [40] of electron recoils in LAr doped with different concentrations oh N_2. The model reproduces precisely the experimental data when an exponential dependence of the radial dimension of the electronic cloud on the nitrogen concentration is assumed, as suggested by measurements in pure liquid nitrogen [41]. The case of low energy nuclear recoils ($E_{kin} < 100$ keV) is peculiar because of the complicate process of the formation and evolution of the electronic cloud, which is taken into account introducing a dependence of the recombination probability on the residual kinetic energy of the recoiling nucleus. The two parameters on which the model depends are extracted through a fitting procedure of the dataset from [46]. The agreement is good over the entire range af electric fields and kinetic energies explored. Finally the model is applied to 5.5 MeV alpha recoils, for which a cylindrical symmetry of the electronic cloud is assumed given that the range is of the order of tens of μm. The three datasets considered: Scalettar *et al.* [37], Gruhn and Edmiston [49], and Andrieux *et al.* [50], show some inconsistencies for electric fields above 5 kV/cm and cannot lead to an unique value of one of the two parameters on which the model depends. The overall agreement of experimental data and the model below 5 kV/cm is good. The problem of charge recombination is a complex one, which is worth of being deeply investigated, since it could be beneficial for next generation experiments for neutrino and dark matter detection.

ACKNOWLEDGMENTS

This work was supported by FAPESP (Fundação de Amparo à Pesquisa do Estado de São Paulo) with the Grant No. 2021/13757-9 and by CNPq (Conselho Nacional de Desenvolvimento Científico e Tecnológico) with the Grant No. 309071/2022-4. The author warmly thanks Ana Machado for inspiring this work, for her precious suggestions and constant support.

APPENDIX A: DERIVATION OF EXTRACTION PROBABILITY EQUATION FOR CYLINDRICAL AND SPHERICAL SYMMETRIES

Secondary electrons produced by the passage of a ionizing particle in liquid argon can travel significant distances, since the energy of the first excited state is around 11.5 eV and atomic argon does not have a vibrational structure which can efficiently absorb energies of few eV. The range of these secondary electrons can be of the order of several hundreds of nm [25]. Electrons emitted with energies above 11.5 eV are reduced to a subexcitation level very fast (∼1 ps).

If the kinetic energy of the primary particle is high enough, the ionization track has a cylindrical symmetry with a thin core of positive ions (diameter of the order of tens of nm) and an extended cloud of secondary electrons which reaches up a radial dimension, r_0, of hundreds of nm after their thermalization [26]. Assuming that the energy spectrum of these secondary electrons is approximately flat between zero and 11.5 eV [27] and that their range depends linearly on their kinetic energy, as in the case of low energy δ rays [51], the number of thermalized electrons in any cylindrical shell, concentric to the primary track of thickness dx and width dr, is constant for any fixed position along the track. In this case the electric field of the cylindrical distribution, $\vec{\mathcal{E}}_c$, is radial and has an intensity of

$$\mathcal{E}_c(r) = \frac{\lambda}{2\pi\epsilon_{LAr}} \times \left(\frac{1}{r} - \frac{1}{r_0}\right) = \mathcal{E}_0 \times \left(\frac{r_0}{r} - 1\right) \tag{A1}$$

where λ is the linear density of positive charges and $\mathcal{E}_0 = \lambda/(2\pi\epsilon_{LAr} r_0)$. The dependence on the position has been omitted, but both $\mathcal{E}_c$ and λ are local quantities which depend on the coordinate along the track.

Considering the application of an external electric field, $\mathcal{E}$, orthogonal to the direction of the ionizing track and neglecting any consideration about the relative track-field orientation, one assumes that the fraction of ionization electrons which can be extracted is the one falling outside the cylinder of radius r_c defined by the relation $\mathcal{E} = \mathcal{E}_c(r_c)$. Noting that this fraction corresponds to the extraction probability P, and that $P = 1 - r_c/r_0$, Eq. (A1) can be written as

$$\frac{\mathcal{E}}{\mathcal{E}_0} = \frac{P}{1-P} \tag{A2}$$

that can be inverted to give P as a function of the applied electric field and of the local ionization density

$$P = \frac{1}{\frac{\mathcal{E}_0}{\mathcal{E}} + 1} = \frac{\mathcal{E}}{k_c \frac{dq_i}{dx} + \mathcal{E}} \tag{A3}$$

where $dq_i/dx = \lambda/e$, $k_c = e/(2\pi\epsilon_{LAr}r_0)$ and e is the electron charge. Electrons are extracted from the direction opposite to the external field, while the remaining fraction of the electronic cloud rearranges itself to maintain an approximately cylindrical symmetry. The external electric field will be effective in extracting electrons until when $\mathcal{E} > \mathcal{E}_c(r_c)$ and eventually all electrons lying outside the cylinder of radius r_c are extracted.

In the limit of a ionization track with a length shorter than the linear dimensions of the electronic cloud, similar arguments can be made to derive the relation between the extraction probability and the external electric field. Assuming an approximately spherical distribution of the electronic cloud and a charge density profile $\propto 1/r$, as in the case of cylindrical distribution, Eq. (A2) still holds, while Eq. (A3) becomes

$$P = \frac{\mathcal{E}}{k_s Q_i + \mathcal{E}} \tag{A4}$$

where Q_i is the total number of ionization electrons and $k_s = e/(4\pi\epsilon_{LAr}r_0^2)$.

The arguments presented in this section should be regarded as a semi-quantitative description of the recombination process and a partial justification of the microscopic model adopted in this work. A complete treatment should include a precise description of the expansion and of the thermalization processes, of the charge distribution inside the electronic cloud and of its geometrical configuration.

APPENDIX B: FIT OF ELECTRON RECOIL DATA AT 59.6 KEV FROM RED PROJECT

The ReD project collected a set of data of electronic recoils produced by the conversion of 59.6 keV γ rays emitted by a ^{241}Am radioactive source with a dual phase LAr chamber [23]. Experimental points have been fitted with Eq. (14) with three free parameters: k, γ, and w_i. The fit is shown in Fig. 8 and the values of the parameters can be found in Table V. Despite the fit reproducing almost perfectly the experimental data, the value of k and γ are smaller than what found in Sec. III A for higher energy recoils (see Table I), while w_i is compatible with the reference value of 23.6 eV. This discrepancy, especially in the value of k, could be attributed to two main circumstances. First, the energy of the recoils is not too far from the low energy threshold of about 10 keV, where Eq. (14) is no more valid and this is not taken into account in the fitting procedure. Second, the number of experimental points is limited and the electric field reaches just 1 kV/cm, differently from the three datasets considered in Sec. III A.

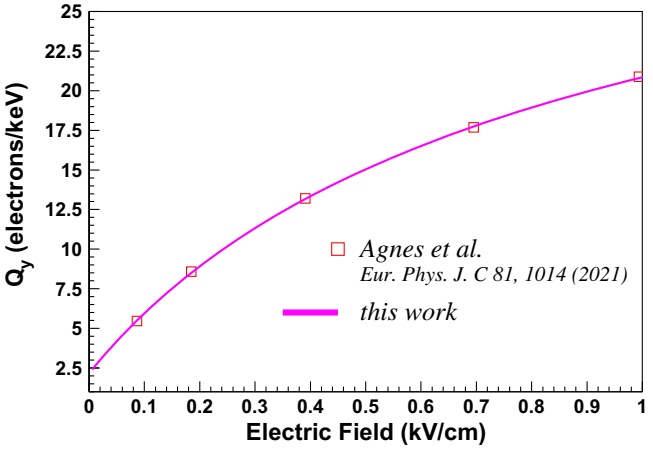

FIG. 8. Charge yield for electron recoils produced by the photoconversion of 59,6 keV γ rays emitted by a ^{241}Am radioactive source. Magenta line represents the result of the fit with the model described in Sec. III A. Data are taken from [23] (ReD project). Error bars have not been reported since they are very small.

TABLE V. Parameters k, γ, and w_i extracted through the fitting procedure of the dataset collected by the ReD project [23].

k (mV)	γ (μm^{-1})	w$_i$ (eV)
(2.2 ± 0.1)	2.2 ± 0.2	24.0 ± 1.0

[1] DUNE Collaboration, Volume I. Introduction to DUNE, J. Instrum. **15**, T08008 (2020).
[2] P. A. Machado, O. Palamara, and D. W. Schmitz, The short-baseline neutrino program at Fermilab, Annu. Rev. Nucl. Part. Sci. **69**, 363 (2019).
[3] H. Chen *et al.* (MicroBooNE Collaboration), Proposal for a new experiment using the booster and NuMI neutrino beamlines: MicroBooNE (2007), https://inspirehep.net/literature/776376.
[4] R. Acciarri *et al.*, The WArP experiment, J. Phys. Conf. Ser. **203**, 012006 (2010).
[5] P. Benetti, R. Acciarri, F. Adamo, B. Baibussinov, M. Baldoceolin, M. Belluco, F. Calaprice, E. Calligarich, M. Cambiaghi, and F. Carbonara, First results from a dark matter search with liquid argon at 87k in the Gran Sasso underground laboratory, Astropart. Phys. **28**, 495 (2008).
[6] C. E. Aalseth, F. Acerbi, P. Agnes, I. F. M. Albuquerque, T. Alexander, A. Alici, A. K. Alton, P. Antonioli, S. Arcelli,

R. Ardito *et al.*, DarkSide-20k: A 20 tonne two-phase LAr TPC for direct dark matter detection at LNGS, Eur. Phys. J. Plus **133**, 131 (2018).
[7] A. Badertscher *et al.* (ArDm Collaboration), Status of the ArDM experiment: First results from gaseous argon operation in deep underground environment, arXiv:1307.0117.
[8] A. Hime, The miniCLEAN dark matter experiment, arXiv:1110.1005.
[9] M. G. Boulay, DEAP-3600 dark matter search at SNOLAB, J. Phys. Conf. Ser. **375**, 012027 (2012).
[10] T. Doke, Fundamental properties of liquid argon, krypton and xenon as radiation detector media, Portugaliae Physica **12**, 9 (1981).
[11] S. Amoruso *et al.*, Analysis of the liquid argon purity in the ICARUS t600 TPC, Nucl. Instrum. Methods Phys. Res., Sect. A **516**, 68 (2004).
[12] DUNE-Collaboration, Volume IV. The DUNE far detector single-phase technology, J. Instrum. **15**, T08010 (2020).
[13] M. Szydagis, A review of basic energy reconstruction techniques in liquid xenon and argon detectors for dark matter and neutrino physics using NEST. Instruments **5**, 13 (2021).
[14] C. Rubbia *et al.*, Underground operation of the ICARUS t600 LAr-TPC: First results, J. Instrum. **6**, P07011 (2020).
[15] W. Walkowiak, Drift velocity of free electrons in liquid argon, Nucl. Instrum. Methods Phys. Res., Sect. A **449**, 288 (2000).
[16] A. Machado and E. Segreto, Arapuca a new device for liquid argon scintillation light detection, J. Instrum. **11**, C02004 (2016).
[17] C. Regenfus, The argon dark matter experiment, *Proceedings of the 4th Patras Workshop on Axions, WIMPs and WISPs, PATRAS 2008* (DESY, Hamburg, 2009), Vol. 203.
[18] P. Agnes *et al.*, Search for low-mass dark matter WIMPs with 12 ton-day exposure of DarkSide-50, Phys. Rev. D **107**, 063001 (2023).
[19] G. Jaffé, Zur theorie der ionisation in kolonnen, Ann. Phys. (Berlin) **347**, 303 (1913).
[20] L. Onsager, Initial recombination of ions, Phys. Rev. **54**, 554 (1938).
[21] J. Thomas and D. A. Imel, Recombination of electron-ion pairs in liquid argon and liquid xenon, Phys. Rev. A **36**, 614 (1987).
[22] P. Agnes *et al.*, Calibration of the liquid argon ionization response to low energy electronic and nuclear recoils with DarkSide-50, Phys. Rev. D **104**, 082005 (2021).
[23] P. Agnes, S. Albergo, I. Albuquerque *et al.*, Performance of the ReD TPC, a novel double-phase lar detector with silicon photomultiplier readout, Eur. Phys. J. C **81**, 1014 (2021).
[24] S. Amoruso *et al.*, Study of electron recombination in liquid argon with the ICARUS TPC, Nucl. Instrum. Methods Phys. Res., Sect. A **523**, 275 (2004).
[25] M. Wojcik and M. Tachiya, Electron thermalization and electron–ion recombination in liquid argon, Chem. Phys. Lett. **379**, 20 (2003).
[26] M. Wojcik, Electron recombination in low-energy nuclear recoils tracks in liquid argon, J. Instrum. **11**, P02005 (2016).
[27] M. Foxe, C. Hagmann, I. Jovanovic, A. Bernstein, K. Kazkaz, V. Mozin, S. Pereverzev, S. Sangiorgio, and P. Sorensen, Low-energy (< 10 keV) electron ionization and recombination model for a liquid argon detector, Nucl. Instrum. Methods Phys. Res., Sect. A **771**, 88 (2015).
[28] M. Foxe, C. Hagmann, I. Jovanovic, A. Bernstein, T. Joshi, K. Kazkaz, V. Mozin, S. Pereverzev, S. Sangiorgio, and P. Sorensen, Modeling ionization and recombination from low energy nuclear recoils in liquid argon, Astropart. Phys. **69**, 24 (2015).
[29] L. Romero, R. Santorelli, E. Sánchez García, T. Lux, M. Leyton, S. di Luise, P. García Abia, R. López Manzano, J. M. Cela-Ruiz, S. Quizhpi, and V. Pesudo, Experimental study of the positive ion feedback from gas to liquid in a dual-phase argon chamber and measurement of the ion mobility in argon gas, Universe **8**, 134 (2022).
[30] R. Acciarri *et al.*, A study of electron recombination using highly ionizing particles in the argoneut liquid argon TPC, J. Instrum. **8**, P08005 (2013).
[31] M. Miyajima, T. Takahashi, S. Konno, T. Hamada, S. Kubota, H. Shibamura, and T. Doke, Average energy expended per ion pair in liquid argon, Phys. Rev. A **9**, 1438 (1974).
[32] M. J. Berger, J. S. Coursey, M A. Zucker, and J. Chang, ESTAR, PSTAR, and ASTAR: Computer Programs for Calculating Stopping-Power and Range Tables for Electrons, Protons, and Helium Ions (version 1.2.3) (2005).
[33] S. Kubota, A. Nakamoto, T. Takahashi, T. Hamada, E. Shibamura, M. Miyajima, K. Masuda, and T. Doke, Recombination luminescence in liquid argon and in liquid xenon, Phys. Rev. B **17**, 2762 (1978).
[34] T. Doke, K. Masuda, and E. Shibamura, Estimation of absolute photon yields in liquid argon and xenon for relativistic (1 MeV) electrons, Nucl. Instrum. Methods Phys. Res., Sect. A **291**, 617 (1990).
[35] A. Hitachi, T. Doke, and A. Mozumder, Luminescence quenching in liquid argon under charged-particle impact: Relative scintillation yield at different linear energy transfers, Phys. Rev. B **46**, 11463 (1992).
[36] This approximation is reasonably well verified since the minimum value of $\frac{dq_i/dx}{\gamma}$ is 4 for E = 1 MeV with the value of γ returned by the fitting procedure and reported in Table I.
[37] R. T. Scalettar, P. J. Doe, H. J. Mahler, and H. H. Chen, Critical test of geminate recombination in liquid argon, Phys. Rev. A **25**, 2419 (1982).
[38] E. Aprile, W. H.-M. Ku, J. Park, and H. Schwartz, Energy resolution studies of liquid argon ionization detectors, Nucl. Instrum. Methods Phys. Res., Sect. A **261**, 519 (1987).
[39] A. Ereditato, M. Hess, S. Janoŝ, I. Kreslo, L. Martinez, M. Messina, U. Moser, B. Rossi, H. U. Shütz, and M. Zeller, Study of ionization signals in a TPC filled with a mixture of liquid argon and nitrogen, J. Instrum. **3**, P10002 (2008).
[40] M. Zeller, I. Badhrees, S. Delaquis, A. Ereditato, S. Janos, I. Kreslo, M. Messina, U. Moser, and B. Rossi, Ionization signals from electrons and alpha-particles in mixtures of liquid argon and nitrogen—perspectives on protons for gamma resonant nuclear absorption applications, J. Instrum. **5**, P10009 (2010).
[41] G. Ramanan and G. R. Freeman, Electron thermalization distances and free ion yields in liquid nitrogen from 77 K to near Tc, J. Chem. Phys. **87**, 319 (1987).
[42] J.-P. Dodelet, K. Shinsaka, and G. R. Freeman, Molecular structure effects on electron ranges and mobilities in liquid hydrocarbons: Chain branching and olefin conjugation: Mobility model, Can. J. Chem. **54**, 744 (1976).

[43] J. F. Ziegler, M. Ziegler, and J. Biersack, Srim—the stopping and range of ions in matter (2010), Nucl. Instrum. Methods Phys. Res., Sect. B **268**, 1818 (2010).
[44] J. Lindhard, V. Nielsen, M. Scharff, and P. V. Thomsen, Integral equations governing radiation effects (notes on atomic collisions, III), Kgl. Danske Videnskab., Selskab. Mat. Fys. Medd.
[45] A. Hitachi and A. Mozumder, Properties for liquid argon scintillation for dark matter searches, arXiv:1903.05815.
[46] H. Cao *et al.* (SCENE Collaboration), Measurement of scintillation and ionization yield and scintillation pulse shape from nuclear recoils in liquid argon, Phys. Rev. D **91**, 092007 (2015).
[47] F. D. Stacey, The ionization of liquid argon by alpha-particles, Aust. J. Phys. **11**, 158 (1958).
[48] Nuclear effects are relevant only at energies below 50 keV. For α particles in the range of few MeV the amount of energy transferred to the nuclei of the medium is negligible.
[49] C. R. Gruhn and M. D. Edmiston, Geminate recombination of α-particle-excited carriers in liguid argon, Phys. Rev. Lett. **40**, 407 (1978).
[50] M. Andrieux, J. Collot, P. de Saintignon, A. Ferrari, J. Hostachy, and P. Martin, Response of an α source mounted in a liquid argon ionization cell and read out in full charge collection mode, Nucl. Instrum. Methods Phys. Res., Sect. A **427**, 568 (1999).
[51] J. J. Butts and R. Katz, Theory of RBE for heavy ion bombardment of dry enzymes and viruses, Radiat. Res. **30**, 855 (1967).